an oily residue which was partitioned between H_2O/CH_2Cl_2. Purification of this crude product in CH_2Cl_2 solution was accomplished as in the synthesis of **16**. In this way a 4-g fraction of the tetra(2,3-dimethoxybenzoyl) compound, **19**, was obtained for use in the next step.

Using the same procedure as in the synthesis of **6**, the following reagents were combined: precursor **19** (4 g, 4.6 mmol); BBr_3 (4.2 mL, 44 mmol); CH_2Cl_2 (115 mL). Hydrolysis (50 mL, H_2O), filtration, and thorough water wash, then vacuum drying at room temperature over P_2O_5/NaOH pellets, gave crude 3,4,3-LICAM (**20**, 3 g), satisfactory for the sulfonation step.

As in the synthesis of **19**, the following reagents were combined: 20 (2.5 g, 3.3 mmol) and 3% fuming H_2SO_4 (30 mL). After pouring on ice, then neutralization with 10 N NaOH to pH 4 and subsequent workup as for **18**, hygroscopic, white solid **21**·6.5H_2O (2.1 g, 50%) was obtained: IR 3700-2500 (>CH, -OH), 1640-1590 (-CON<), 1470, 1420, 1380, 1210-1180 (SO_3^-), 1100, 1040, 615 (SO_3^-) cm^{-1}; NMR δ 1.3-2.3 (broad, 8 H, $-CH_2CH_2N<$), 2.8-3.8 (broad, 12 H, $-CH_2N<$), 7.1-7.9 (broad m, 8 H, ArH).

Anal. Calcd for $C_{38}H_{38}N_4O_{24}S_4Na_4\cdot 6.5H_2O$ (variable water content): C, 35.88; H, 4.04; N, 4.40; S, 10.08; Na, 7.23. Found: C, 36.38; H, 3.73; N, 4.24; S, 9.26; Na, 7.13.

Acknowledgments. We are pleased to acknowledge the assistance of Dr. P. W. Durbin and Ms. Sarah Jones in the biological evaluation of these compounds. We also thank Dr. A. Avdeef for experimental assistance. This work was supported by the Division of Nuclear Sciences, Office of Basic Energy Sciences, U.S. Department of Energy, under Contract No. W-7405-ENG-48.

References and Notes

(1) Part 2 in this series: Sofen, S. R.; Abu-Dari, K.; Freyberg, D. P.; Raymond, K. N. *J. Am. Chem. Soc.* **1978**, *100*, 7882-7887.
(2) Catsch, A. "Radioactive Metal Mobilization in Medicine"; Charles C Thomas: Springfield, Ill., 1964.
(3) Stoves, B. J.; Atherton, D. R.; Buster, D. S. *Health Phys.* **1971**, *20*, 369.
(4) Foreman, H.; Moss, W.; Langham, W. *Health Phys.* **1960**, *2*, 326.
(5) Durbin, P. *Health Phys.* **1975**, *29*, 495, and references cited therein.
(6) Weitl, F. L.; Raymond, K. N.; Smith, W. L.; Howard, T. R. *J. Am. Chem. Soc.* **1978**, *100*, 1170-1172.
(7) Neilands, J. B., Ed. "Microbial Iron Metabolism"; Academic Press: New York, 1974.
(8) Schmidt, H. U.S. Patent 1 889 383; *Chem. Abstr.* **1933**, *27*, 1363. U.S. Patent 1 988 576; *Chem. Abstr.* **1935**, *29*, 1588.
(9) The structures, as well as our abbreviated nomenclature for some of the title compounds, appear in Table I. For IUPAC names see Experimental Section. Our system of abbreviation, based on CAM as an acronym for catechoylamide, uses prefixes CY and LI to indicate a cyclic or linear compound, respectively. The numbers in the prefix indicate the length of the methylene chains connecting the CAM moieties and, should letters appear in the prefix, they indicate N-terminal substituents in a linear compound. The suffix indicates substituents on each benzene ring of the CAM ligand.
(10) For a discussion of the direct sulfonation of aromatic hydrocarbons, see: Adams, R., Ed. "Organic Reactions", Vol. 3; Wiley: New York, 1946; pp 141-197.
(11) The two highest symmetry coordination geometries for eight coordination are D_{4d} (Archimedian antiprism) or D_{2d} (trigonal-faced dodecahedron). We have found the latter in the $[Ac(cat)_4]^{4-}$ structures (see ref 1 and 12).
(12) Sofen, S. R.; Cooper, S. R.; Raymond, K. N. *Inorg. Chem.* **1979**, *18*, 1611-1616.
(13) Durbin, P. W.; Jones, E. S.; Raymond, K. N.; Weitl, F. L. *Radiat. Res.*, in press.
(14) Weitl, F. L.; Raymond, K. N. *J. Am. Chem. Soc.* **1979**, *101*, 2728-2731.

Preparation, Physical Properties, and X-ray Structure of the Mixed-Valence Compound Diferrocenylselenium Iodine Triiodide Hemi(methylene chloride)

Jack A. Kramer,[1] Frank H. Herbstein,*[2] and David N. Hendrickson*[1]

Contribution from the School of Chemical Sciences, University of Illinois, Urbana, Illinois 61801, and the Department of Chemistry, Technion-Israel Institute of Technology, Haifa, Israel. *Received September 28, 1979*

Abstract: Diferrocenyl selenide is oxidized by iodine in dichloromethane to give a mixed-valence compound. The structure of $\{[Fe(\eta^5\text{-}C_5H_5)(\eta^5\text{-}C_5H_4)]_2Se\}I_3\cdot I_2\cdot{}^1/_2CH_2Cl_2$ has been determined using heavy-atom methods in conjunction with least-squares refinement of data measured on a four-circle X-ray diffractometer. The compound crystallizes with triclinic symmetry with two formula weights in a cell having the dimensions a = 11.647 (5) Å, b = 11.519 (5) Å, c = 10.633 (5) Å, α = 97.65 (4)°, β = 95.73 (4)°, γ = 88.10 (4)°, and V = 1406.5 Å^3. The observed and calculated densities are 2.60 and 2.658 g cm^{-3}, respectively. The structure was refined using 3582 observed reflections (graphite-monochromated Mo Kα) to give conventional discrepancy factors of R = 0.0616 and R_w = 0.0654. Discrete mixed-valence $[Fe(\eta^5\text{-}C_5H_5)(\eta^5\text{-}C_5H_4)]_2Se^+$ cations and an anion structure consisting of zigzag chains of triiodide anions and iodine molecules are present. The mixed-valence bridged ferrocene cation assumes a gauche conformation intermediate between the cisoid and transoid conformations. The distance between the two iron ions is 6.058 (2) Å. As indicated by the centroid-to-centroid ring distances, the two $Fe(\eta^5\text{-}C_5H_5)(\eta^5\text{-}C_5H_4)$ moieties are structurally different. One is a ferrocenyl group, the other a ferricenyl group. The localized nature of the mixed-valence cation is substantiated by ^{57}Fe Mössbauer spectra, which show two quadrupole-split doublets. EPR data are inconclusive, whereas IR spectra also point to a localized electronic structure. No intervalence transfer band is seen in the near-IR region of the electronic absorption spectrum of this compound and it is concluded that it is a class I mixed-valence species.

Introduction

Mixed-valence compounds contain ions of the same element in two different oxidation states.[3-6] The study of mixed-valence compounds will potentially aid in understanding electron transfer as found in oxidation-reduction, electrochemical, and biological processes. There is a growing interest in the low-energy electronic absorption band, the so-called intervalence band, exhibited by mixed-valence compounds. A detailed analysis of this absorption band could provide information about thermal electron transfer.[7-9]

Bridged ferrocenes have proven to be good candidates for mixed-valence compounds owing to their variability in structure and suitability for study with several physical techniques such as ^{57}Fe Mössbauer spectroscopy and EPR.[10,11] By employing the intrinsic time scales associated with various physical techniques, it has been possible to bracket the thermal electron-transfer rates for the mixed-valence bridged ferro-

0002-7863/80/1502-2293$01.00/0

Table I. Crystal Data

$[(C_5H_5)Fe(C_5H_4)Se(C_5H_4)Fe(C_5H_5)]^+I_2 \cdot I_3^- \cdot \frac{1}{2}(CH_2Cl_2)$	
$C_{20.5}H_{19}Fe_2SeI_5Cl$	mol wt 1126.01
	$F(000)$ 1024
a = 11.647(5) Å	α = 97.65(4)°
b = 11.519(5) Å	β = 95.73(4)°
c = 10.633(5) Å	γ = 88.10(4)°
d_m = 2.60 g cm^{-3} (flotation in *sym*-tetrabromoethane-toluene mixture)	
d_c = 2.658 cm^{-3} for Z = 2	V = 1406.5 Å^3
	μ(Mo Kα) = 74.88 cm^{-1}

cenes. To date, only two basic types of compounds have been noted. There are those that have been characterized to be relatively localized with thermal electron-transfer rates that are less than the reciprocal of the ^{57}Fe Mössbauer time scale, that is, less than ca. 10^7 s^{-1}. This group includes the salts of biferrocene$^+$ (I),[10-12] [1.1]ferrocenophane$^+$ (II),[13] and diferrocenylacetylene$^+$ (III).[14,15] The other type of mixed-valence

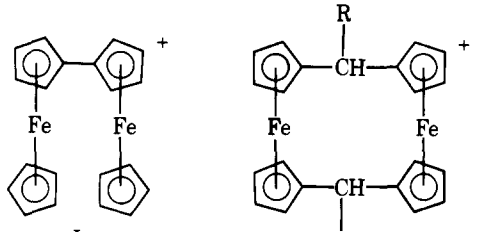

I

R = H, CH_3

II

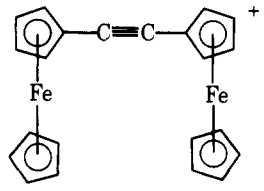

III

bridged ferrocene is apparently delocalized on all spectroscopic time scales. The salts of bis(fulvalene)diiron$^+$ (IV),[10,16] 1′,6′-diiodobiferrocene$^+$ (V),[10] and [2.2]ferrocenophane-1,13-diyne$^+$ (VI)[14,15] have been shown to be delocalized on the

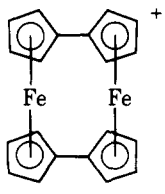

IV

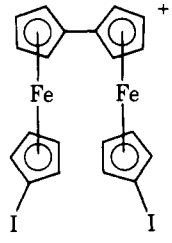

V

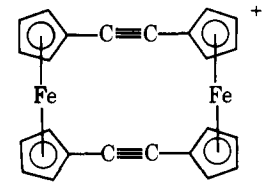

VI

^{57}Fe Mössbauer time scale and also delocalized on the EPR time scale, which would mean that the thermal electron-transfer rate is greater than ca. 10^{10} s^{-1}. The bis(fulvalene) diiron$^+$ species has also been indicated to have equivalent iron ions on the X-ray PES time scale.[16] The factors that determine the thermal electron-transfer rate for a given mixed-valence bridged ferrocene have not been unambiguously established. The results of very recent magnetic Mössbauer work[17] were taken to indicate that the delocalized species, i.e., those with equivalent iron ions, are in fact largely organic radicals.

The X-ray crystal structure of only one mixed-valence ferrocene, ferricenyl(III)tris(ferrocenyl(II))borate, has been reported.[18] The centroid-to-centroid distance between the two cyclopentadienyl rings in one -(η^5-C_5H_4)(η^5-C_5H_5)Fe moiety was found to be longer than the corresponding distances in the other three metallocene moieties. Unfortunately, no ^{57}Fe Mössbauer, EPR, or spectroscopic data other than electronic absorption have been reported as yet for this compound.

In 1976, Cowan et al.[19] reported the preparation and some physical properties of diferrocenyl selenide (VII). Despite an

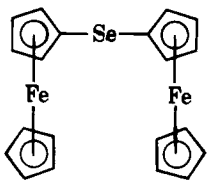

VII

appreciable difference of 0.22 V between the two one-electron oxidation half-waves, no intervalence transfer transition was observed in the electronic absorption spectrum of a solution containing the mixed-valence monocation. No mixed-valence compounds were isolated.

This study began with efforts to prepare a salt of mixed-valence diferrocenyl selenide$^+$. Herein are reported the physical properties and single-crystal X-ray structure of the triiodide salt of diferrocenyl selenide.

Experimental Section

Compound Preparation. A sample of diferrocenyl selenide was prepared according to the literature procedure.[19] Elemental analyses were performed by the staff of the Microanalytical Laboratory of the School of Chemical Sciences, University of Illinois. Anal. Calcd for $C_{20}H_{18}Fe_2Se$: C, 53.50; H, 4.04; Fe, 24.88. Found: C, 53.25; H, 4.09; Fe, 24.51.

The triiodide salt, $\{[Fe(\eta^5\text{-}C_5H_5)(\eta^5\text{-}C_5H_4)]_2Se\}I_3 \cdot I_2 \cdot \frac{1}{2}CH_2Cl_2$, was prepared by dissolving 0.276 g (2.17 mmol) of iodine in 100 mL of freshly dried and distilled CH_2Cl_2. This solution was added to a stirred solution of 0.178 g (0.396 mmol) of diferrocenyl selenide in 20 mL of CH_2Cl_2. The resulting solution was filtered and then allowed to evaporate slowly. Large, black crystals which were suitable for X-ray diffraction were obtained. Anal. Calcd for $C_{20}H_{18}Fe_2SeI_5 \cdot \frac{1}{2}CH_2Cl_2$: C, 21.87; H, 1.70; Fe, 9.92; I, 56.35; Cl, 3.15. Found: C, 21.82; H, 1.75; Fe, 9.88; I, 56.54; Cl, 3.46.

Physical Methods. Variable-temperature (4.2-290 K) magnetic susceptibilities were measured with a PAR Model 150A vibrating-sample magnetometer as described in a previous paper.[20] Iron-57 Mössbauer spectra were obtained at 77 and 4.2 K with an instrument which has been described.[21] Computer fittings of the ^{57}Fe Mössbauer data to Lorentzian lines were carried out with a modified version of a previously reported program.[22]

Infrared spectra were recorded with a Perkin-Elmer Model 283 spectrophotometer. Samples were prepared as 13-mm KBr pellets. A Cryogenics Technology, Inc., "Spectrim" closed-cycle helium gas refrigerator equipped with KBr windows was used to record low-temperature (ca. 30 K) infrared spectra. Electronic absorption spectra of 13-mm KBr pellets of the compounds were recorded with a Cary 14 spectrophotometer.

EPR spectra were obtained with a Varian E-9 X-band spectrometer equipped with a Varian temperature controller (80-350 K). Spectra at 2.8 K were recorded by employing an Oxford Instruments helium-flow accessory.[23]

Crystal Measurements. The crystals are deeply colored rhombs. Preliminary photography showed that the crystal symmetry was triclinic and that the measured density and unit cell volume were consistent with the proposed molecular formula.

A crystal was sealed into a thin-walled glass capillary and mounted on a Phillips PW1100 four-circle diffractometer. Crystal data are given in Table I. The intensities of over 3600 reflections were measured (graphite-monochromated Mo Kα, $\omega/2\theta$ scan, scan speed 0.05°ω s^{-1}, scan width 1.20°ω, background counted for 12 s at each of the scan extremities). Corrections were made for Lorentz and polarization factors, but not for absorption.

Solution and Refinement of Structure. The crystal structure was solved via the Patterson function, assuming V-shaped I_5^- ions [d(I-I) = 3.0 Å and ∠I-I-I = 90° at the apex]. Two possible solutions were found, one of which descended to a false minimum with R = 42%, while the second refined smoothly, using difference syntheses and

Table II. Atomic Parameters for Chlorines of CH_2Cl_2 ($\times 10^4$)[a]

atom	*x*	*y*	*z*	occupancy	U_{iso}, Å^2
Cl(A)	3416(6)	−37(8)	5106(8)	1/2	860
Cl(B)	5917(8)	−210(17)	5377(18)	1/4	860
Cl(C)	5905(12)	−40(35)	4837(44)	1/8	860
Cl(D)	5796(14)	330(34)	4628(41)	1/8	860

[a] Occupancy and isotropic Debye-Waller factor not refined.

least-squares methods in concert, to the final solution. The SHELX-76 program set was used. During the refinement it soon became clear that zigzag chains of intereacting I_2 molecules and I_3^- ions were present, and not discrete I_5^- ions.

The difference density in the region of the methylene chloride molecule was interpreted in terms of six different orientations (related in pairs across the center of symmetry at 1/2, 0, 1/2) of the Cl · · · Cl vector, which was constrained to a distance of 2.935 (10) Å, in accordance with the microwave spectroscopy results for CH_2Cl_2.[24] On the basis of the difference maps, the chlorine atoms were given individual occupancy factors and equal isotropic temperature factors; these were not refined. Details are given in Table II. The methylene chloride carbon atom was not located nor, a fortiori, were the hydrogen atoms.

The cyclopentadienyl groups of the ferrocenyl moieties, after having been located by successive difference syntheses, were inserted in idealized geometries [regular pentagons with d(C-C) = 1.42 Å and d(C-H) = 1.08 Å] at the penultimate cycle of refinement and allowed to relax in the final cycle (anisotropic carbon thermal parameters, isotropic for the hydrogen atoms). The final R value was 0.0616 (R_w = 0.0654) and the refined weighting factor was $w(F) = 0.65/(\sigma^2(F) + 0.0032F^2)$. This indicates that the experimentally determined standard deviations of the $F(hkl)$ were underestimated by a factor of ca. 1.24. Atomic coordinates are given in Table III, while the Debye-Waller factors and the structure factor lists are found in the supplementary material.

Despite the relatively low R factor, ripples of up to 1.4 e Å^{-3} were found on the final difference synthesis. These appeared around the heavy atoms (I, Se, Fe), showing that the thermal motion had not been accounted for; presumably the lack of absorption corrections and the disorder of the CH_2Cl_2 molecules also contribute to the noise in the electron-density maps. This noise and the large thermal motion of the cyclopentadienyl rings are responsible for the poor precision of the hydrogen-atom positions.

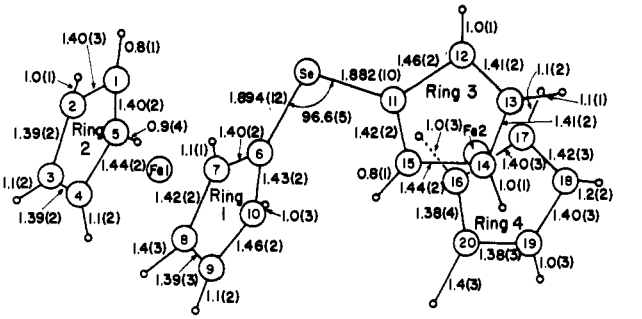

Figure 1. The diferrocenylselenium cation, projected onto (001) and showing nomenclature, bond lengths, and one bond angle (for other angles see Table IV). The esd's of the bond angles in the rings: ring 1, ~1.4°; ring 2, ~1.1°; ring 3, ~1.1°; ring 4, ~1.8°

Results and Discussion

Description of the Molecular Structure. The single-crystal X-ray structure of $\{[Fe(\eta^5\text{-}C_5H_5)(\eta^5\text{-}C_5H_4)]_2Se\}I_3 \cdot I_2 \cdot {}^1/_2CH_2Cl_2$ was solved by heavy-atom techniques. Interatomic distances and bond angles are given in Table IV. The compound proved to be a pentaiodide salt of the bridged ferrocene cation $[Fe(\eta^5\text{-}C_5H_5)(\eta^5\text{-}C_5H_4)]_2Se^+$. The atom numbering used for this cation and some bond lengths and angles are shown in Figure 1. An ORTEP stereoscopic view of the same cation is given in Figure 2.

The conformation and dimensions of the diferrocenyl selenide cation in part determine the rate of the thermal electron transfer in this mixed-valence cation. As can be seen in Figure 1, the angle at the Se atom is 96.6 (5)°. Ring 3 is essentially coplanar with the Se and C(6) atoms, while the angle between ring 1 and 3 (see Table V) is 90.0° (alternatively, τ[C(7)-C(6)-Se-C(11)] = −90.8(1.1)° and τ[C(6)-Se-C(11)-C(12)] = −178.0(8)°). Thus, the mixed-valence cation can be described as having the metallocene moiety comprised of rings 1 and 2 rotated by 90° out of the plane containing C(6), Se, and ring 3 of the second metallocene moiety. This gauche conformation is intermediate between the (very unlikely) cisoid conformation and the transoid conformation, the later of which is found in diferrocenyl ketone[25] and

Table III. Atomic Coordinates ($\times 10^4$)[a]

atom	*x*	*y*	*z*	atom	*x*	*y*	*z*
I(1)	960(1)	3790(1)	4305(1)	C(16)	9485(15)	657(14)	7434(28)
I(2)	2326(1)	2103(1)	2668(1)	C(17)	10487(21)	445(12)	8213(17)
I(3)	3582(1)	491(1)	968(1)	C(18)	11438(14)	825(14)	7649(18)
I(4)	6249(1)	1952(1)	2153(1)	C(19)	10979(16)	1311(14)	6568(17)
I(5)	8389(1)	2786(1)	3123(1)	C(20)	9796(21)	1188(19)	6437(22)
C(1)	4436(11)	3256(17)	8834(15)	H(1)	449(9)	318(9)	959(10)
C(2)	4048(11)	4351(13)	8509(15)	H(2)	437(11)	509(11)	904(11)
C(3)	3604(10)	4201(14)	7232(15)	H(3)	325(19)	490(20)	669(20)
C(4)	3732(11)	3027(14)	6740(15)	H(4)	382(19)	257(20)	581(20)
C(5)	4237(11)	2419(13)	7759(16)	H(5)	434(12)	165(12)	754(13)
Fe(1)	5292(1)	3695(1)	7395(1)	H(7)	675(7)	557(7)	833(8)
C(6)	7004(9)	3682(12)	7916(11)	H(8)	561(22)	576(22)	595(23)
C(7)	6623(10)	4815(12)	7719(13)	H(9)	584(18)	320(20)	493(21)
C(8)	6129(12)	4782(17)	6441(14)	H(10)	661(22)	204(22)	684(24)
C(9)	6227(10)	3638(18)	5839(13)	H(12)	1024(7)	286(7)	1082(7)
C(10)	6736(11)	2901(15)	6769(15)	H(13)	1211(9)	335(10)	969(10)
Se	7713(1)	3233(1)	9465(1)	H(14)	1140(9)	430(9)	770(10)
C(11)	9244(8)	3466(9)	9151(11)	H(15)	910(8)	406(9)	753 (9)
C(12)	10259(10)	3145(12)	9958(11)	H(16)	894(24)	82(25)	812(26)
C(13)	11227(10)	3473(13)	9404(14)	H(17)	1075(15)	16(15)	910(16)
C(14)	10871(11)	3914(11)	8250(14)	H(18)	1220(17)	148(17)	785(19)
C(15)	9629(10)	3914(10)	8088(12)	H(19)	1128(23)	176(23)	598(26)
Fe(2)	10329(1)	2220(1)	8145(2)	H(20)	952(20)	185(22)	539(23)

[a] Esd's in units of last significant digit are given in parentheses.

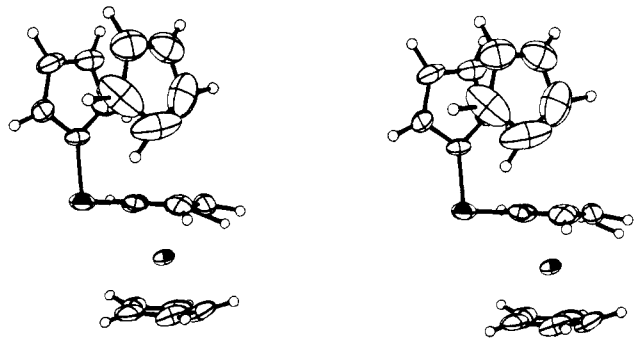

Figure 2. ORTEP stereoview of the diferrocenylselenium cation, viewed in the plane of ring 1. The nonhydrogen atoms are shown as 50% probability ellipsoids. Fe(1) is between the lower pair of rings (1/2) and Fe(2) is barely apparent between the upper (3/4).

in the diferrocenylmethylium cation.[26] It appears that the conformation of the two rings attached to the Se atom is such that nonbonded interactions between hydrogen atoms bonded to α-carbon atoms are minimized. The C(7)-C(15) distance is 3.617 (17) Å and that of C(10)-C(15) is 3.683 (18) Å, which lead to hydrogen-hydrogen contacts of H(7)-H(15) = 3.49 (13) Å and H(10)-H(15) = 3.73 (27) Å.

The Debye-Waller factors of many of the atoms of the cation are large; see Figure 2. As has been observed in other systems,[25,27-30] the thermal motion of the cyclopentadienyl ligand is large in the plane of each ring and is greater for the unsubstituted rings than for the substituted rings. It also appears that the thermal motion of ring 4 is greater than that of ring 2. A suggestion as to the cause of this difference is given below. In any event, high accuracy was not attained for most of the atoms of the two ferrocenyl moieties. This could be due to some disorder caused by the variable packing of the methylene chloride molecules. On the other hand, no significant deviations from regular and planar cyclopentadienide rings are apparent (see Figure 1). In each ferrocenyl moiety, the pairs of rings are not quite coplanar; the angle between rings 1 and 2 is 1.0°, and that between rings 3 and 4 is 4.7°. In both ferrocenyl moieties the rings are essentially eclipsed. The angle of rotation of ring 1 relative to ring 2 averages to ca. 5.5 (8)°, while the analogous angle for rings 3 and 4 is 3.3 (4)°.

According to Wheatley,[31] 1.43 Å is a representative C-C(ring) bond length which generally appears shortened owing to in-plane librational motion. The effect is apparent in the C-C bond lengths of rings 2 and 4, which have average C-C bond distances of 1.404 (22) and 1.394 (30) Å, respectively. Rings 1 and 3 are experiencing less thermal motion, and their average C-C bond distances of 1.420 (22) and 1.427 (21) Å, respectively, are more normal.

The centroid-to-centroid (c-t-c) distance between rings 1 and 2 is 3.277 (19) Å. This is slightly less than that observed for ferrocene[32,33] and several other ferrocene derivatives.[25,34,35] The c-t-c distance between rings 3 and 4 is 3.397 (22) Å. Such an increase in c-t-c distance has been observed when ferrocenes are oxidized to the corresponding ferricenium ions.[36,37] It is clear, then, that in $[Fe(\eta^5\text{-}C_5H_5)(\eta^5\text{-}C_5H_4)]_2Se^+$ the group consisting of Fe(1) and rings 1 and 2 is the ferrocenyl group, while Fe(2) and its associated rings have been oxidized to form the ferricenyl group. Cowan et al.[18] were also able to identify the one ferricenyl group in ferricenyl(III)tris(ferrocenyl(II))borate by differences in c-t-c distances. The increased Fe-ring distances in the Fe(2) ferricenyl group of $[Fe(\eta^5\text{-}C_5H_5)(\eta^5\text{-}C_5H_4)]_2Se^+$ indicate that the removal of the e_{2g} ($d_{x^2-y^2}$, d_{xy}) electron from the Fe(2) metallocene led to a weakening of the Fe-C(ring) bonds. This could explain the greater thermal motion in ring 4 compared to ring 2.

The Fe ions in the mixed-valence cation are very slightly displaced from the lines joining the centroids of the bonded cyclopentadienide rings. The centroid(1)-Fe(1)-centroid(2) angle is 177.9 (7)°. The analogous angle for the Fe(2) group is 177.2 (8)°.

The two selenium-iron distances in $[Fe(\eta^5\text{-}C_5H_5)(\eta^5\text{-}C_5H_4)]_2Se^+$ are significantly different [Se-Fe(1) = 3.471 (2) Å and Se-Fe(2) = 3.578 (2) Å]. The distance between the two iron ions is 6.058 (2) Å. The closest Se-I contact is 6.817 (2) Å between the Se and I(5) atoms. The atoms I(1), I(2), and I(4) are nearest to Fe(1) with Fe-I distances ranging from 5.74 to 5.92 Å. The only Fe(2)-I distance less than 7.5 Å is that to I(5) at 5.698 (2) Å.

Table IV. Interatomic Distances (Å) and Angles (deg) for $\{[Fe(\eta^5\text{-}C_5H_5)(\eta^5\text{-}C_5H_4)]_2Se\}I_3\cdot I_2\cdot\frac{1}{2}CH_2Cl_2$[a]

Distances			
C(1)-C(2)	1.401(24)	C(11)-C(12)	1.457(16)
C(2)-C(3)	1.394(22)	C(12)-C(13)	1.408(17)
C(3)-C(4)	1.392(23)	C(13)-C(14)	1.409(21)
C(4)-C(5)	1.434(22)	C(14)-C(15)	1.440(17)
C(5)-C(1)	1.399(24)	C(15)-C(11)	1.420(17)
C(6)-C(7)	1.400(19)	C(16)-C(17)	1.396(31)
C(7)-C(8)	1.418(20)	C(17)-C(18)	1.419(28)
C(8)-C(9)	1.393(27)	C(18)-C(19)	1.396(26)
C(9)-C(10)	1.430(21)	C(19)-C(20)	1.381(31)
C(10)-C(6)	1.430(21)	C(20)-C(16)	1.376(35)
Fe(1)-C(1)	2.033(15)	Fe(2)-C(11)	2.131(11)
Fe(1)-C(2)	2.026(14)	Fe(2)-C(12)	2.082(13)
Fe(1)-C(3)	2.029(12)	Fe(2)-C(13)	2.068(15)
Fe(1)-C(4)	2.019(14)	Fe(2)-C(14)	2.056(13)
Fe(1)-C(5)	2.046(14)	Fe(2)-C(15)	2.096(12)
Fe(1)-C(6)	2.016(11)	Fe(2)-C(16)	2.094(19)
Fe(1)-C(7)	2.023(13)	Fe(2)-C(17)	2.057(14)
Fe(1)-C(8)	2.040(16)	Fe(2)-C(18)	2.074(17)
Fe(1)-C(9)	2.062(13)	Fe(2)-C(19)	2.053(18)
Fe(1)-C(10)	2.017(14)	Fe(2)-C(20)	2.085(25)
C(1)-H(1)	0.8(1)	C(16)-H(16)	1.0(3)
C(2)-H(2)	1.0(1)	C(17)-H(17)	1.1(2)
C(3)-H(3)	1.1(2)	C(18)-H(18)	1.2(2)
C(4)-H(4)	1.1(2)	C(19)-H(19)	1.0(3)
C(5)-H(5)	0.9(4)	C(20)-H(20)	1.4(3)
C(7)-H(7)	1.1(1)	C(12)-H(12)	1.0(1)
C(8)-H(8)	1.4(3)	C(13)-H(13)	1.1(1)
C(9)-H(9)	1.1(2)	C(14)-H(14)	1.0(1)
C(10)-H(10)	1.0(3)	C(15)-H(15)	0.8(1)
Se-C(6)	1.894(12)	I(1)-I(2)	2.9639(16)
Se-C(11)	1.881(9)	I(2)-I(3)	2.8826(16)
Se-Fe(1)	3.4716(16)		
Se-Fe(2)	3.5773(18)	I(3)-(4)	3.6151(16)
Fe(1)-Fe(2)	6.0585(17)		
		I(4)-I(5)	2.7533(16)
centroid(1)-Fe(1)	1.634(13)	centroid(3)-Fe(2)	1.697(13)
centroid(2)-Fe(1)	1.643(13)	centroid(4)-Fe(2)	1.700(19)
centroid(1)-centroid(2)	3.277(19)	centroid(3)-centroid(4)	3.397(22)
Angles			
C(1)-C(2)-C(3)	108.1(1.3)	C(11)-C(12)-C(13)	106.7(1.0)
C(2)-C(3)-C(4)	108.8(1.3)	C(12)-C(13)-C(14)	109.9(1.2)
C(3)-C(4)-C(5)	107.4(1.3)	C(13)-C(14)-C(15)	107.6(1.1)
C(4)-C(5)-C(1)	107.0(1.3)	C(14)-C(15)-C(11)	107.7(1.0)
C(5)-C(1)-C(2)	108.6(1.4)	C(15)-C(11)-C(12)	107.9(1.0)
C(6)-C(7)-C(8)	108.5(1.2)	C(16)-C(17)-C(18)	107.8(1.7)
C(7)-C(8)-C(9)	108.2(1.3)	C(17)-C(18)-C(19)	106.5(1.5)
C(8)-C(9)-C(10)	108.7(1.3)	C(18)-C(19)-C(20)	108.7(1.7)
C(9)-C(10)-C(6)	105.4(1.2)	C(19)-C(20)-C(16)	109.0 (1.9)
C(10)-C(6)-C(7)	109.0(1.1)	C(20)-C(16)-C(17)	109.0(1.9)
C(6)-Se-C(11)	96.6(5)	centroid(1)-Fe(1)-centroid(2)	177.9(7)
I(1)-I(2)-I(3)	177.17(5)	centroid(3)-Fe(2)-centroid(4)	177.2(8)
I(2)-I(3)-I(4)	90.69(4)		
I(3)-I(4)-I(5)	172.61(5)		

[a] Atom numbering is given in Figure 1.

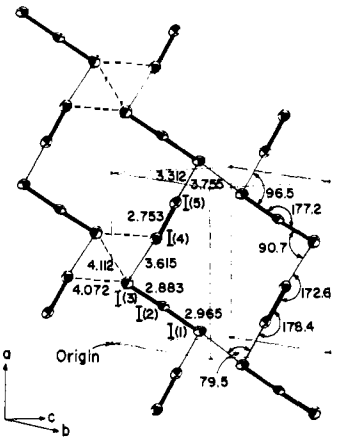

Figure 3. Projection of a single polyiodide layer onto (0$\bar{1}$1). The esd's of the distances are 0.001 Å and of the angles <0.1°. The atoms are shown as 50% probability ellipsoids. The secondary and tertiary interactions between I_2 and I_3^- are shown by thinner lines and the closer van der Waals distances by broken lines.

Table V. Equations of Best Planes of Cyclopentadienyl Rings and Other Groups of Atoms[a]

no. of plane	plane through atoms	*A*	*B*	*C*	*D*, Å
1	C(1)-C(5)	0.9434	0.2349	−0.3790	2.192
2	C(6)-C(10)	0.9371	0.2454	−0.3931	5.363
3	C(11)-C(15)	−0.0477	0.8587	0.3929	6.721
4	C(16)-C(20)	−0.1180	0.8295	0.4354	2.773
5[b]	I(1)-I(5), I(1)A-I(5)A	0.0380	−0.6643	0.8177	0.742

[a] The form of the equation, expressed with respect to crystal axes, is $Ax + By + Cz = D$, where *x*, *y*, *z* are positional coordinates in Å. The interplanar angles: 1 2 1.0°, 2 3 90.0°, 3 4 4.7°, 5 (011) 4.7°. [b] I(1)-I(5) are the reference iodine atoms (coordinates Table III). I(1)A-I(5)A are related to the reference iodines by inversion through ½, ½, ½. The deviations (Å) of the iodines from plane 5: I(1) 0.143, I(2) 0.071, I(3) −0.119, I(4) −0.087, I(5) 0.212. For atoms I(1)-A-I(5)A the deviations have the same values but are of opposite sign.

The Se-C(6) and Se-C(11) bond distances of 1.894 (12) and 1.882 (10) Å, respectively, are significantly shorter than the C(sp^3)-Se bond distances cited by Zaripov et al.,[38] which range between 1.943 (1) and 1.959 (10) Å. According to Karle and Karle,[39] selenium bonds to aromatic carbon atoms are generally shorter than the above C(sp^3)-Se range, with values averaging about 1.93 Å and some distances as short as 1.876 (19) Å.[40] Selenium-carbon double bonds have lengths[39] between 1.82 and 1.87 Å. The short Se-C bond lengths in the present compound may reflect some Se($d\pi$) + C($p\pi$) bonding. Finally, the C(6)-Se-C(11) bond angle of 96.6° in $[Fe(\eta^5\text{-}C_5H_5)(\eta^5\text{-}C_5H_4)]_2Se^+$ is less than those observed in di-*p*-tolyl selenide,[41] where ∠C-Se-C = 106 (2)°, and in diphenyl selenide,[42] where the angle is 107.5 (2.0)°. More nearly similar angles are found in 1,4-diselenatobenzene,[43] where ∠C-Se-C is 94.4 (9)°, and in aliphatic selenium derivatives,[39] which generally have bond angles less than 100°.

The anion consists of zigzag chains of triiodide anions and iodine molecules (Figure 3) and resembles the analogous arrangements in bis(phenacetin) hydrogen iodine triiodide[44] and quinuclidinium iodine triiodide.[45] The respective values of *d*(I-I) are 2.753 (1), 2.752 (2), and 2.74 Å in the I_2 molecules and 2.965 (1), 2.883 (1), 2.906 (2), and 2.92 Å in the I_3^- ions. In all three salts the I-I bond length in the I_2 part is increased over the vapor-phase value for I_2 (2.662 Å).[46] A clear-cut explanation for the variation of I-I distances in the I_3^- ions is not obvious. The ten iodine atoms in the unit cell lie within 0.21 Å of a plane, which is inclined at 4.7° to (0$\bar{1}$1) (Table V). The reference I_3^- ion and I_2 molecule are slightly inclined, in opposite directions, to the best plane through all the iodines.

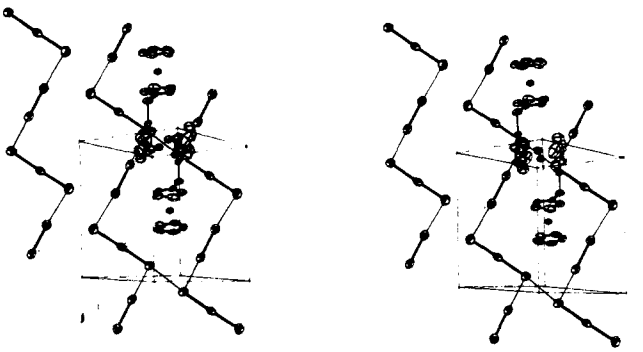

Figure 4. Stereoview of crystal structure viewed approximately normal to (0$\bar{1}$1). For clarity only a single cation is shown above and below the polyiodide layer. The orientation of the diagram is similar to that in Figure 3.

Essentially isolated V-shaped I_5^- ions have been found in a KI_3/KI_5 complex of valinomycin[47] and in bis(α-benzyldioximato)di(β-picoline)iron(III) pentaiodide;[48] interacting V-shaped, I_5^- ions have been found in $N(CH_3)_4I_5$.[49,50]

Molecular Packing. The structure as a whole can be described in terms of cationic and anionic layers, lying approximately parallel to (0$\bar{1}$1). The anionic layer is composed of zigzag chains of I_2 and I_3^- moieties, the chain direction being parallel to [100]; these chains are bonded by tertiary interactions, approximately in the [311] direction, between centrosymmetrically related I_3^- ions. The weaker in-chain interaction is not much stronger than the between-chain interaction, insofar as the strengths of these interactions can be represented by the I- - -I distances of 3.615 and 3.755 Å. The rather bulky and awkwardly shaped cations form layers parallel to and interleaved with the polyiodide layers; with this arrangement a void is left about the center of symmetry at (½ 0 ½) and this is filled by the disordered methylene chloride molecule (one per unit cell), which has been only approximately located in the structure analysis.

This type of arrangement—alternating cationic and anionic layers—is quite common among the polyiodide salts, being found in $(phenacetin)_2 \cdot HI_5$ and $(theobromine)_2 \cdot H_2I_8$.[44] A particularly close resemblance between overall structures is shown by quinuclidinium pentaiodide[45] and the present structure; the location of cation with respect to polyiodide layer is very similar in both compounds (cf. Figure 4 of the present paper and Figure 1 of ref 45).

Comparison of Polyiodide Layers in Three Polyiodide Salts. The arrangements of I_2 and I_3^- moieties in $(phenacetin)_2 \cdot HI_5$, the present compound, and quinuclidinium·HI_5 show interesting variations on a common basic theme. We consider the zigzag I_2- - -I_3^- chain as the primary structural unit, with tertiary interactions between I_3^- moieties next in importance and then van der Waals interactions. This hierarchy is based on the differences of ca. 0.2 Å between the characteristic I- - -I distances found for the various interactions; although description is facilitated by definite distinctions between the interactions, it is much more likely that the differences are gradual rather than sharp. The arrangement of the chains is illustrated schematically in Figure 5 (see Figure 13 of ref 51). In $(phenacetin)_2 \cdot HI_5$ all chains are translationally equivalent, with only van der Waals interactions between them. In diferrocenylselenium pentaiodide hemi(methylene chloride) parallel ribbons are formed by two adjacent chains, with interactions between centrosymmetrically related I_3^- moieties. There are only van der Waals interactions between adjacent ribbons. A ribbon is made up of almost square, centrosymmetric units

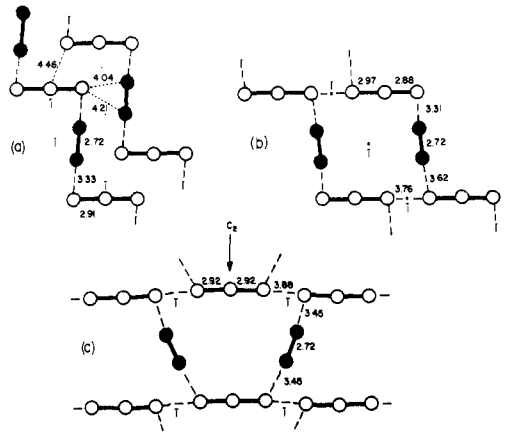

Figure 5. Schematic comparison of the polyiodide layers in (a) (phenacetin)$_2$·HI$_5$; (b) bis(ferrocenyl)selenium·I$_5$·½CH$_2$Cl$_2$; (c) quinuclidinium pentaiodide.

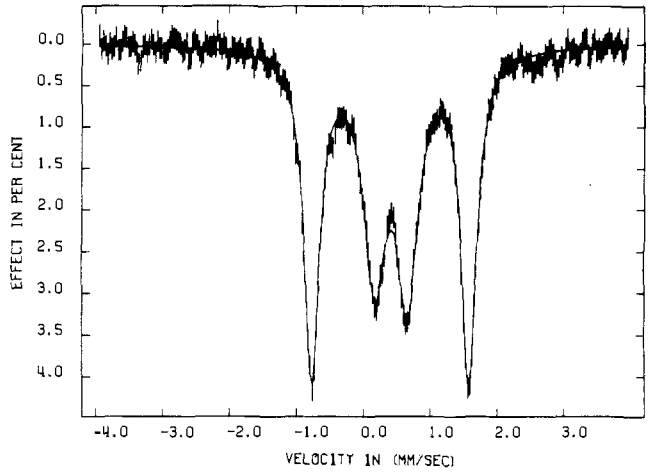

Figure 6. ^{57}Fe Mössbauer spectrum at 90 K of {[Fe(η^5-C$_5$H$_5$)(η^5-C$_5$H$_4$)]$_2$Se}I$_3$·I$_2$·½CH$_2$Cl$_2$. The isomer shift is referenced to iron metal.

(Figure 5b). The interacting V-shaped I_5^- ions of $N(CH_3)_4I_5$[49,50] are arranged in rather similar squares which repeat in *two* dimensions to form a planar network. In quinuclidinium pentaiodide the zigzag chain has a cisoid (Figure 5c) rather than a transoid conformation (Figures 5a and 5b) about the I_3^- ions. In this compound the chains in a layer are translationally equivalent and have a twofold axis normal to their axes of extension. Each I_3^- moiety is linked at its ends to two adjacent I_3^- moieties by tertiary interactions (d(I- - -I) = 3.88 Å). The repeat unit has a trapezoidal form. In all these structures I atoms of I_2 are bicoordinated; in (quinuclidinium)·HI$_5$ both outer iodines are tricoordinated, in {[Fe(η^5-C$_5$H$_5$)(η^5-C$_5$H$_4$)]$_2$Se}I$_3$·I$_2$·½CH$_2$Cl$_2$ one is tricoordinated and one bicoordinated, and both are bicoordinated in (phenacetin)$_2$·HI$_5$.

^{57}Fe Mössbauer Spectroscopy. Mössbauer spectroscopy is a particularly useful technique for probing the electronic states of the iron ions in mixed-valence bridged ferrocenes. Ferrocene[52] and ferrocenyl[10,11a,14,53] groups give spectra characterized by large quadrupole splittings in the range of 2.0–2.5 mm/s, while the spectra of the ferricenium ion[52] and ferricenyl groups[53,54] are characterized by small or vanishing quadrupole splittings.

Mössbauer spectra were recorded for {[Fe(η^5-C$_5$H$_5$)(η^5-C$_5$H$_4$)]$_2$Se}I$_3$·I$_2$·½CH$_2$Cl$_2$ at 90 and 4.2 K. There is essentially no temperature dependence. The 90 K spectrum is shown in Figure 6. The various absorption peaks in each spectrum were least squares fit to Lorentziam lines and the resulting fitting parameters are summarized in Table VI together with data for related molecules. It is clear from Figure 6 that two equal-area quadrupole-split doublets are seen in the spectrum. The outer doublet of the 90 K spectrum has a quadrupole splitting (ΔE_Q) of 2.346 (3) mm/s and an isomer shift (δ) of 0.520 (4) mm/s relative to iron metal; the corresponding values for the inner doublet are 0.495 (5) and 0.529 (7) mm/s, respectively. The major conclusion from this Mössbauer spectrum is that the mixed-valence ion [Fe(η^5-C$_5$H$_5$)(η^5-C$_5$H$_4$)]$_2$Se$^+$ is localized on the ^{57}Fe Mössbauer time scale. The thermal electron-transfer rate is less than ca. 10^7 s^{-1}.

Mössbauer data were also obtained for [Fe(η^5-C$_5$H$_4$)(η^5-C$_5$H$_4$)]$_2$Se. The unoxidized molecule at room temperature gives a single doublet with ΔE_Q = 2.342 (6) mm/s and δ = 0.439 (8) mm/s vs. iron metal. Thus, the quadrupole splitting of the ferrocenyl doublet for the mixed-valence compound is the same as that for the unoxidized molecule. An increase of ca. 0.1 mm/s in δ values is commonly observed in the Mössbauer spectra of ferrocence systems cooled from room temperature to liquid-nitrogen temperature. Efforts were made to prepare a dioxidized salt of diferrocenyl selenide by oxidation with DDQ (2,3-dichloro-5,6-dicyano-1,4-benzoquinone) in CH_2Cl_2. An analytically pure sample was not obtained; there was always contamination by monooxidized material. Nevertheless, a room-temperature Mössbauer spectrum was run for one sample of {[Fe(η^5-C$_5$H$_5$)(η^5-C$_5$H$_4$)]$_2$Se}(DDQH)$_2$, where DDQH is the monoanion of the hydroquinone. A doublet with ΔE_Q = 0.494 (14) mm/s and δ = 0.417 (20) mm/s was seen. It is interesting that the ΔE_Q value for this dioxidized salt is very close to that for the ferricenyl doublet for the mixed-valence compound.

[Fe(η^5-C$_5$H$_5$)(η^5-C$_5$H$_4$)]$_2$Se$^+$ is unique in mixed-valence ferrocenes, because it does not show an intervalence transfer band in the near-IR region (vide infra) as has been observed for other mixed-valence ferrocenes. There is very little interaction between the ferrocenyl and ferricenyl moieties in [Fe(η^5-C$_5$H$_5$)(η^5-C$_5$H$_4$)]$_2$Se$^+$. This is interesting in view of the fact that the ΔE_Q values for the two different iron ions in this mixed-valence species are essentially equal to those found for the unoxidized and dioxidized samples of this bridged ferrocene. It has been noted[18,43] that the quadrupole splitting of the ferrocenyl moiety of biferricenium picrate is ca. 0.3 mm/s *less* than the ΔE_Q value for ferrocene, and the ferricenyl moiety of this same compound has a ΔE_Q value that is ca. 0.3 mm/s *greater* than observed for the ferricenium ion. As can be seen in Table VI, this is also found for the triiodide salts of biferrocene and diferrocenylacetylene. These three salts of mixed-valence bridged ferrocenes do exhibit some degree of interaction between the ferrocenyl and ferricenyl moieties in them. It is suggested that the change of ΔE_Q values seen for the mixed-valence ferrocenes that are localized on the Mössbauer time scale is a reflection of the weak interaction between the Fe(II) and Fe(III) ions. The mixed-valence diferrocenyl selenide ion experiences the weakest such interaction.

EPR and Magnetic Susceptibility. The magnetic susceptibility of {[Fe(η^5-C$_5$H$_5$)(η^5-C$_5$H$_4$)]$_2$Se}I$_3$·I$_2$·½CH$_2$Cl$_2$ was measured between 4.2 and 270 K. The data are illustrated in Figure 7 and are given in the supplementary material. The effective magnetic moment (μ_{eff}) per molecule (or equivalently per ferricenyl moiety) is plotted as a function of temperature in Figure 7. For comparison purposes, the data for ferricenium triiodide are also plotted. The μ_{eff} value of the diferrocenyl selenide mixed-valence salt varies from 2.52 μ_B at 270 K to 2.02 μ_B at 4.2 K. It can be seen that this behavior parallels that seen for ferricenium triiodide and consequently there is no sign of an *inter*molecular magnetic exchange interaction in the mixed-valence salt.

X-Band EPR spectra were recorded for several samples of {[Fe(η^5-C$_5$H$_5$)(η^5-C$_5$H$_4$)]$_2$Se}I$_3$·I$_2$·½CH$_2$Cl$_2$ at 77 and 2.8

Table VI. ^{57}Fe Mössbauer Fitting Parameters for Diferrocenyl Selenide and Related Compounds[a]

compd	T, K	ΔE_Q	δ[b]	Γ[c]
$[Fe(\eta^5\text{-}C_5H_5)(\eta^5\text{-}C_5H_4)]_2Se$	RT	2.342(6)	0.439(8)	0.314(10), 0.308(10)
$\{[Fe(\eta^5\text{-}C_5H_5)(\eta^5\text{-}C_5H_4)]_2Se\}I_3\cdot I_2\cdot{}^1/_2CH_2Cl_2$	90	2.346(3)	0.520(4)	0.138(3), 0.136(3)
		0.495(5)	0.529(7)	0.206(5), 0.190(4)
	4.2	2.331(4)	0.528(5)	0.142(3), 0.150(3)
		0.488(5)	0.538(7)	0.190(4), 0.192(5)
$\{[Fe(\eta^5\text{-}C_5H_5)(\eta^5\text{-}C_5H_4)]_2Se\}(C_8HN_2O_2Cl_2)_2$[d]	RT	0.494(14)	0.417(20)	0.680(18), 0.662(18)
$(\eta^5\text{-}C_5H_5)Fe(\eta^5\text{-}C_5H_4)(\eta^5\text{-}C_5H_4)Fe(\eta^5\text{-}C_5H_5)$[e] (biferrocene)	78	2.36	0.52	
$[(\eta^5\text{-}C_5H_5)Fe(\eta^5\text{-}C_5H_4)(\eta^5\text{-}C_5H_4)Fe(\eta^5\text{-}C_5H_5)]I_3$[f]	4.2	2.119(3)	0.519(3)	0.308(4), 0.268(4)
		0.381(3)	0.531(3)	0.303(4), 0.303(4)
$[(\eta^5\text{-}C_5H_5)Fe(\eta^5\text{-}C_5H_4)(\eta^5\text{-}C_5H_4)Fe(\eta^5\text{-}C_5H_5)](BF_4)_2$[g]	77	0.163	0.497	
$(\eta^5\text{-}C_5H_5)Fe(\eta^5\text{-}C_5H_4\text{-}C{\equiv}C\text{-}\eta^5\text{-}C_5H_4)Fe(\eta^5\text{-}C_5H_5)$[h] (diferrocenylacetylene)	78	2.41	0.50	
$[(\eta^5\text{-}C_5H_5)Fe(\eta^5\text{-}C_5H_4\text{-}C{\equiv}C\text{-}\eta^5\text{-}C_5H_4)Fe(\eta^5\text{-}C_5H_4)]I_3$[h]	78	2.18	0.54	
		0.49	0.50	
$[(\eta^5\text{-}C_5H_5)Fe(\eta^5\text{-}C_5H_4\text{-}C{\equiv}C\text{-}\eta^5\text{-}C_5H_4)Fe(\eta^5\text{-}C_5H_5)]I_6$[i]	77	0.222(6)	0.506(8)	0.538(14), 0.368(6)
$(\eta^5\text{-}C_5H_5)_2Fe$	78[h]	2.39	0.52	
	77[j]	2.40	0.475	
$[(\eta^5\text{-}C_5H_5)_2Fe]I_3$[h]	78	0.00	0.53	

[a] ΔE_Q, δ, and Γ are given in mm/s. Error in least significant figure is given in parentheses. [b] Isomer shift relative to iron metal. [c] Full width at half-height; the line at the more negative velocity is listed first. [d] $C_8HN_2O_2Cl_2^-$ is the monoanion of 2,3-dicyano-5,6-dichloro-*p*-hydrobenzoquinone. The greater than normal widths observed for this compound are most likely due to additional weak shouldering absorptions from a small impurity of the monooxidized compound. [e] Reference 53. [f] Reference 10. [g] Reference 11a. [h] Reference 14. [i] J. A. Kramer and D. N. Hendrickson, unpublished results. [j] Reference 52.

Table VII. Transitions Observed in Electronic Absorption Spectra[a]

$[Fe(\eta^5\text{-}C_5H_5)(\eta^5\text{-}C_5H_4)]_2Se$		$\{[Fe(\eta^5\text{-}C_5H_5)(\eta^5\text{-}C_5H_4)]_2Se\}I_3\cdot I_2\cdot{}^1/_2CH_2Cl_2$	
this work, $\times 10^3$ cm^{-1}	lit.,[b] $\times 10^3$ cm^{-1} (L M^{-1})	this work, $\times 10^3$ cm^{-1}	lit.,[c] $\times 10^3$ cm^{-1} (L M^{-1})
22.7	22.7 (440)	11.5	11.6 (1350)
37.7	37.7 (1000)	19.6	
45.5	44.1 (18 500	24.4	
	44.6 (18 000)	33.3	
		37.0	
		45.5	

[a] KBr pellets. [b] Reference 19, acetonitrile solution. [c] Reference 19, observed for acetonitrile solution containing mixed-valence ion.

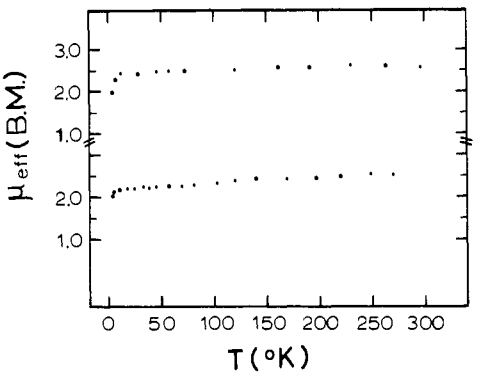

Figure 7. Effective magnetic moment per ferric ion (μ_{eff} in μ_B) for $\{Fe(\eta^5\text{-}C_5H_5)(\eta^5\text{-}C_5H_4)]_2Se\}I_3\cdot I_2\cdot{}^1/_2CH_2Cl_2$ (upper) and $[Fe(\eta^5\text{-}C_5H_5)_2]I_3$ (lower).

K. The data are at the same time puzzling and disappointing. Little temperature dependence was noted and each spectrum consisted of one strong derivative-like signal at $g = 2.13$–2.16. Three other less intense features at $g = 3.3$–3.5, 1.83, and 1.46–1.49 consistently appeared, but these signals had intensities that varied somewhat from one sample to another. A mixed-valence bridged ferrocene which is localized on the EPR time scale has a large g-tensor anisotropy with $g_\parallel$ ranging between 3.62 and 4.17 and $g_\perp$ between 1.47 and 1.76. The EPR-delocalized species show $g_\parallel$ values in the range of 2.3–2.8 and $g_\perp$ close to 2.0.[10] It is not possible to conclude from the EPR data whether the mixed-valence selenium system is localized or delocalized. There are at least two possible explanations for the complexity of the EPR spectra for this compound. Although very crystalline samples were used, the requisite sample grinding and the evacuation of the EPR tube could have pulled off some of the I_2 from the sample. It is also quite possible that there exists in this compound a weak *inter*molecular magnetic exchange interaction, too weak to be seen in the susceptibility at 4.2 K. This type of interaction could exchange average the signal expected for a single molecule.

Electronic Absorption Spectroscopy. Cowan et al.[19] reported the solution spectrum of diferrocenyl selenide and the partial spectra of the mixed-valence monocation and of the dication. No intervalence transfer transition was noted in the near-IR for the mixed-valence species in solution. It was also found that the $^2E_{2u} \leftarrow {}^2E_{2g}$ transition which occurs at 16.2×10^3 cm^{-1} in the spectrum of the ferricenium ion is shifted to 11.6×10^3 cm^{-1} (ϵ 1350) for the mixed-valence species. The shift was attributed to the inductive effect of the selenium atom.

Electronic absorption spectra were run for KBr-pelleted disks of $[Fe(\eta^5\text{-}C_5H_5)(\eta^5\text{-}C_5H_4)]_2Se$ and $\{[Fe(\eta^5\text{-}C_5H_5)(\eta^5\text{-}C_5H_4)]_2Se\}I_3\cdot I_2\cdot{}^1/_2CH_2Cl_2$. The data are given in Table VII. As can be seen, the data obtained for the solid sample of the unoxidized species are similar to those reported by Cowan,[19] except for poorer resolution of the higher energy bands in the KBr-pellet spectrum.

The solid-state spectrum for the pentaiodide salt of the mixed-valence species is of interest, particularly because it was only possible to clearly identify the 11.6×10^3 cm^{-1} band for the mixed-valence species in acetonitrile. A band at 11.5×10^3 cm^{-1} is seen in the solid-sample spectrum of the mixed-valence salt. It was shown that *n*-butylferricenyl selenide shows an analogous band at 11.0×10^3 cm^{-1}; thus the selenium atom is the origin of the shift of the $^2E_{2u} \leftarrow {}^2E_{2g}$ transition. The bands observed at 19.6, 33.3, and 45.5×10^3 cm^{-1} in the KBr-pellet spectrum of the mixed-valence salt are probably due to transitions associated with $I_3^- I_2$.[55] The bands at 24.4, 37.0, and 45.5×10^3 cm^{-1} are most likely attributable to the ferrocenyl moiety of the mixed species.[56] In short, it appears that the electronic absorption spectrum of the mixed-valence salt is essentially a superposition of the features for the ferro-

Figure 8. The 775–900-cm^{-1} region of the IR spectrum of KBr pellets of $[Fe(\eta^5\text{-}C_5H_5)(\eta^5\text{-}C_5H_4)]_2Se$ (upper) and $\{[Fe(\eta^5\text{-}C_5H_5)(\eta^5\text{-}C_5H_4)]_2Se\}I_3\cdot I_2\cdot{}^1/_2CH_2Cl_2$ (lower).

cenyl and ferricenyl moieties. Thus, $\{[Fe(\eta^5\text{-}C_5H_5)(\eta^5\text{-}C_5H_4)]_2Se\}I_3\cdot I_2\cdot{}^1/_2CH_2Cl_2$ is most likely localized on the electronic spectroscopy time scale.

Infrared Spectroscopy. Infrared spectroscopy should be useful in determining whether a given mixed-valence ferrocene species has an electron-transfer rate greater than or less than ca. 10^{13} s^{-1}. To date, no such study has been reported. The spectra of diferrocenyl selenide and its mixed-valence triiodide salt were run as KBr pellets. The data are summarized in Table VIII.

The major bands[57] in the IR spectrum of ferrocene are found at 475, 491, 817, 1005, 1111, 1412, and 3085 cm^{-1}. The first two bands are due to a ring–metal–ring stretch and a tilt. The next two bands are assignable to perpendicular and parallel C–H bends, respectively. The 1111-cm^{-1} band is due to the asymmetric ring-breathing vibration, and the 1412-cm^{-1} band is due to the asymmetic C–C stretch. The C–H stretch band is found at 3085 cm^{-1}. Basically, the same bands are seen for diferrocenyl selenide; however, because there are both substituted and unsubstituted rings, splitting is seen in some of the bands.

When ferrocene is oxidized to the ferricenium ion, the ring–metal–ring stretch and tilt bands are greatly reduced in intensity.[57] Less pronounced losses in intensity are seen for other bands. The band system that appears to be the most diagnostic of the state of a given ferrocene moiety is the perpendicular C–H bend, which is seen at 815 cm^{-1} for ferrocene. This band shifts to 851 cm^{-1} for ferricenium triiodide, but, what is even more important, the band remains relatively intense in going from ferrocene to the oxidized salt. We have found this band to be a useful indicator of the oxidation state of the iron ions of biferrocene-type compounds. In a latter paper,[58] it will be shown that the position and multiplicity of this band can be used to ascertain whether a given mixed-valence bridged ferrocene is localized or delocalized on the IR time scale.

Figure 8 illustrates the IR spectra of $[Fe(\eta^5\text{-}C_5H_5)(\eta^5\text{-}C_5H_4)]_2Se$ and the I_3^- salt of the mixed-valence cation in the region of 775–900 cm^{-1}. It can be seen that, in going from the unoxidized molecule to the mixed-valence species, new perpendicular C–H bending vibrations appear at higher energy than observed for the unoxidized molecule. At the same time, the spectrum of the mixed-valence species still exhibits C–H bending bands at 818 and 832 cm^{-1} that are attributable to a ferrocenyl group. The mixed-valence species simultaneously shows perpendicular C–H bending bands for ferrocenyl and ferricenyl groups. The electron-transfer rate is slower than the IR time scale, as indicated by Mössbauer spectroscopy.

Table VIII. Infrared Spectral Data for $[Fe(\eta^5\text{-}C_5H_5)(\eta^5\text{-}C_5H_4)]_2Se$ (A) and for $\{[Fe(\eta^5\text{-}C_5H_5)(\eta^5\text{-}C_5H_4)]_2Se\}I_3\cdot I_2\cdot{}^1/_2CH_2Cl_2$ (B)[a]

A	B	A	B
352 sh	350 vw	1001 ms	1001 ms
365 m	366 vw		1007 m
407 w	397 vw	1013 sh	1012 sh
419 vw	419 vw	1017 ms	1019 sh
420 br, sh	420 w, br	1024 ms	1022 ms
488 s	486 vs	1028 sh	
500 s	497 vs		1048 m
598 w	600 w	1055 mw	1057 sh
628 m	613 vw	1062 sh	
	697 w	1097 sh	1095 sh
735 vw	732 m	1105 m	1103 m
788 sh	788 sh	1138 sh	1140 sh
810 s	807 sh	1148 m	
819 s	818 m	1153 m	1153 m
824 sh	829 sh	1190 w	1196 vw
832 m	832 s	1204 w	
	840 s	1234 w	
844 w	846 sh	1258 w	1265 vw
853 sh	861 mw	1344 w	1335 w
866 w	865 mw	1361 w	1358 vw
878 m	877 mw		1372 w
885 sh		1387 m	1384 vw
894 vw	894 vw	1409 m	1408 s
	920 vw	1780 w	
		3083 m	3090 w
		3100 sh	

[a] The frequencies are given in cm^{-1}. Relative intensities of the bands: vs = very strong, s = strong, ms = medium strong, m = medium, mw = medium weak, w = weak, vw = very weak, sh = shoulder, br = broad. Both samples were run as KBr pellets.

Conclusions and Comments

The results of various physical techniques indicate that the pentaiodide salt of the monocation of diferrocenyl selenide is a class I mixed-valence compound with localized, noninteracting ferrocenyl and ferricenyl groups. The X-ray structure shows that the centroid-to-centroid distance of the ferricenyl groups is 0.12 Å greater than that of the ferrocenyl group in $\{[Fe(\eta^5\text{-}C_5H_5)(\eta^5\text{-}C_5H_4)]_2Se\}I_3\cdot I_2\cdot{}^1/_2CH_2Cl_2$. Two-quadrupole-split doublets are seen in the ^{57}Fe Mössbauer spectrum, which indicates that the electron-transfer rate is less than ca. 10^7 s^{-1}. Infrared and electronic absorption data also indicate a localized structure, whereas EPR data are inconclusive. No intervalence transfer band is seen in the near-infrared region of the electronic absorption spectrum of the mixed-valence triiodide salt.

It is interesting to compare the structure and properties of the triiodide salt of the diferrocenyl selenide monocation with those[18] of ferricenyl(III)tris(ferrocenyl(II))borate. Both of these mixed-valence species have saturated bridging atoms, and have nearly the same differences in centroid-to-centroid distances of the ferrocenyl and ferricenyl groups. In spite of this, only the latter compound exhibits an intervalence transfer absorption band in the near-infrared region, which indicates that there is an interaction between the ferrocenyl and ferricenyl groups only in the mixed-valence borate species. In the PKS vibronic-coupling model[7] for mixed-valence compounds, three parameters are needed to describe the properties of such species. Electronic coupling between the two metal centers is gauged by ϵ, whereas the vibronic coupling is gauged by the λ parameter. This latter parameter is directly proportional to the difference in the equilibrium value of the a_{1g} monomer normal coordinate in the two different oxidation states which

characterize the mixed-valence compound. It is unlikely that there is any appreciable difference in vibronic coupling between the mixed-valence borate and diferrocenyl selenide species. A third parameter, W, gauges the difference in zero-point energies for the two states of the mixed-valence species. Presumably W does not change appreciably between these two compounds. A difference in electronic coupling must be present.

It would be expected that electronic coupling *via the bridging group* would be more likely in the selenium-bridged mixed-valence ion, because selenium is more polarizable than boron. The selenium atom also has d orbitals available for bonding interactions with the π system of the cyclopentadienide rings. However, the selenium-bridged mixed-valence ion exhibits a weaker interaction than the boron-bridged species. Thus, the electronic coupling probably depends on a direct interaction between the two iron ions in one mixed-valence cation. The principal factor controlling this type of electronic coupling is, of course, the iron–iron distance, which depends on the relative conformation of the two $Fe(\eta^5\text{-}C_5H_5)(\eta^5\text{-}C_5H_4)$ moieties in the mixed-valence ion. In the mixed-valence borate compound, the positioning of the one ferricenyl group is such that the Fe(III) ion only has a direct sighting with an Fe(II) ion of one of the three ferrocenyl groups. The conformation of these groups is very similar (i.e., gauche with less twist) to that found for the mixed-valence diferrocenyl selenide ion. The relevant Fe(III)–Fe(II) distance in the borate ion is 5.36 Å. On the other hand, the two metallocene moieties in the selenium-bridged ion are twisted somewhat further apart to give an Fe(III)–Fe(II) distance of 6.06 Å and part of the organic shrubbery is interposed between the two iron ions in this ion. This would prevent any direct Fe–Fe interaction.

Acknowledgment. We are grateful to Dr. M. Kapon for some preliminary work. Dr. Herbstein thanks the Deutsche Forschungsgemeinschaft for financial support and Professors F. Cramer and W. Saenger (Max-Planck Institut für Experimentelle Medizin, Göttingen) for their interest. Support was also derived from NIH Grant HL 13652 to Dr. Hendrickson.

Supplementary Material Available: Tables of Debye–Waller factors (Table IX) and structure factors for $\{[Fe(\eta^5\text{-}C_5H_5)(\eta^5\text{-}C_5H_4)]_2Se\}I_3\cdot I_2\cdot\frac{1}{2}CH_2Cl_2$, and the magnetic susceptibility vs. temperature data for this same compound (Table X) (23 pages). Ordering information is given on any current masthead page.

References and Notes

(1) University of Illinois.
(2) Technion-Israel Institute of Technology.
(3) Robin, M. B.; Day, P. *Adv. Inorg. Chem. Radiochem.* **1967**, *10*, 247.
(4) Allen, G. C.; Hush, N. S. *Prog. Inorg. Chem.* **1967**, *8*, 257.
(5) Hush, N. *Prog. Inorg. Chem.* **1967**, *8*, 391.
(6) Parks, R. D., Ed. "Valence Instabilities and Related Narrow-Band Phenomena"; Plenum Press: New York, 1977.
(7) (a) Wong, K. Y.; Schatz, P. N.; Piepho, S. B. *J. Am. Chem. Soc.* **1979**, *101*, 2793. (b) Piepho, S. B.; Krausz, E. R.; Schatz, P. N. *Ibid.* **1978**, *100*, 2996.
(8) Meyer, T. J. *Acc. Chem. Res.* **1977**, *11*, 94.
(9) (a) Hopfield, J. J. *Biophys. J.* **1977**, *18*, 311, and references cited therein. (b) Potosek, M. J.; Hopfield, J. J. *Proc. Natl. Acad. Sci. U.S.A.* **1977**, *74*, 229.
(10) Morrison, W. H. Jr.; Hendrickson, D. N. *Inorg. Chem.* **1975**, *14*, 2331.
(11) (a) Cowan, D. O.; Collins, R. L.; Kaufman, F. *J. Phys. Chem.* **1971**, *75*, 2025. (b) Cowan, D. O.; Candela, G. A.; Kaufman, F. *J. Am. Chem. Soc.* **1970**, *92*, 6198.
(12) Cowan, D. O.; LeVanda, C.; Park, J.; Kaufman, F. *Acc. Chem. Res.* **1973**, *6*, 1, and references cited therein.
(13) Morrison, W. H. Jr.; Hendrickson, D. N. *Chem. Phys. Lett.* **1973**, *22*, 119.
(14) Motoyama, I.; Watanabe, M.; Sano, H. *Chem. Lett.* **1978**, 513.
(15) LeVanda, C.; Cowan, D. O.; Leitch, C.; Bechgaard, K. *J. Am. Chem. Soc.* **1974**, *96*, 6789. LeVanda, C.; Bechgaard, K.; Cowan, D. O. *J. Org. Chem.* **1976**, *41*, 2700.
(16) LeVanda, C.; Bechgaard, K.; Cowan, D. O.; Mueller-Westerhoff, U. T.; Eilbracht, P.; Candela, G. A.; Collins, R. L. *J. Am. Chem. Soc.* **1976**, *98*, 3181.
(17) Rudie, A. W.; Davison, A.; Frankel, R. B. *J. Am. Chem. Soc.* **1979**, *101*, 1629.
(18) Cowan, D. O.; Shu, P.; Hedberg, F. L.; Rossi, M.; Kistenmacher, T. J. *J. Am. Chem. Soc.* **1979**, *101*, 1304.
(19) Shu, P.; Bechgaard, K.; Cowan, D. O. *J. Org. Chem.* **1976**, *41*, 1849.
(20) Morrison, W. H. Jr.; Krogsrud, S.; Hendrickson, D. N. *Inorg. Chem.* **1973**, *12*, 1998.
(21) Münck, E.; Debrunner, P. G.; Tsibris, J. C. M.; Gunsalus, I. C. *Biochemistry* **1972**, *11*, 855.
(22) Chrisman, B. L.; Tumolillo, T. A. *Comput. Phys. Commun.* **1971**, *2*, 322.
(23) Campbell, S. J.; Herbert, I. R.; Warwick, C. B.; Woodgate, J. M. *Rev. Sci. Instrum.* **1976**, *47*, 1172.
(24) Myers, R. J.; Gwinn, W. D. *J. Chem. Phys.* **1952**, *20*, 1420.
(25) Trotter, J.; MacDonald, A. C. *Acta Crystallogr.* **1966**, *21*, 359.
(26) Cais, M.; Dani, S.; Herbstein, F. H.; Kapon, M. *J. Am. Chem. Soc.* **1978**, *100*, 5554.
(27) Krukonis, A. P.; Silverman, J.; Yannoni, N. F. *Acta Crystallogr., Sect. B* **1972**, *28*, 987.
(28) Hall, L. H.; Brown, G. M. *Acta Crystallogr. Sect. B* **1971**, *27*, 81.
(29) Kaluski, Z. L.; Struchkov, Yu. T.; Avoyan, R. L. *J. Struct. Chem.* (*USSR*) **1964**, *5*, 683.
(30) Carter, O. L.; McPhail, A. T.; Sim, G. A. *J. Chem. Soc. A* **1967**, 365.
(31) Wheatley, P. J. "Perspectives in Structural Chemistry", Vol. I; Wiley: New York, 1967.
(32) Bohn, R. K.; Haaland, A. *J. Organomet. Chem.* **1966**, *5*, 470.
(33) Dunitz, J. D.; Orgel, L. E.; Rich, A. *Acta Crystallogr.* **1956**, *9*, 373.
(34) Gibbons, C. S.; Trotter, J. *J. Chem. Soc. A* **1971**, 2659.
(35) Churchill, M. R.; Wormald, J. *Inorg. Chem.* **1969**, *8*, 1970.
(36) Mammano, N. J.; Zalkin, A.; Landers, A.; Rheingold, A. L. *Inorg. Chem.* **1977**, *16*, 297.
(37) Bats, J. W.; deBoer, J. J.; Bright, D. *Inorg. Chim. Acta* **1971**, *5*, 605.
(38) Zaripov, N. M; Golubinski, A. V.; Aichmutova, G.; Vikov, L. V. *Zh. Strukt. Khim.* **1978**, *19*, 894.
(39) Karle, I. L.; Karle, J. "Organic Selenium Compounds: Their Chemistry and Biology", Klayman, D. L., Günther, W. H. H., Eds.; Wiley-Interscience: New York, 1973; p 990.
(40) Balwir, M.; Habres, G.; Dideberg, O.; Dupont, L.; Piette, J. L. *Acta Crystallogr., Sect. B* **1975**, *31*, 2188.
(41) Blackmore, W. R.; Abrahams, S. C. *Acta Crystallogr.* **1955**, *8*, 323.
(42) Marsh, R. E. *Acta Crystallogr.* **1952**, *5*, 458.
(43) McDonald, W. S.; Pettit, L. D. *J. Chem. Soc. A* **1970**, 2044.
(44) Herbstein, F. H.; Kapon, M. *Philos. Trans. R. Soc. London, Ser. A* **1979**, *291*, 199.
(45) Jander, J.; Pritzkow, H.; Trommsdorf, K-U. *Z. Naturforsch. B* **1975**, *30*, 720.
(46) Karle, I. L. *J. Chem. Phys.* **1955**, *23*, 1739.
(47) Neupert-Laves, K.; Dobler, M. *Helv. Chim. Acta* **1975**, *58*, 432.
(48) Dvorkin, A. A.; Simonov, Yu A.; Malinovskii, T. I.; Bulgak, I. I.; Batyr, D. G. *Dokl. Phys. Chem.* (*Engl. Transl.*) **1977**, *234*, 1372.
(49) Hach, R. J.; Rundle, R. E. *J. Am. Chem. Soc.* **1951**, *73*, 4321.
(50) Broekema, J.; Havinga, E. E.; Wiebbnga, E. H. *Acta Crystallogr.* **1957**, *10*, 596.
(51) Tebbe, K. F. In "Homoatomic Rings, Chains and Macromolecules of Main-Group Elements", Rheingold, A. L., Ed.; Elsevier: Amsterdam, 1977; Chapter 24.
(52) Collins, R. L. *J. Chem. Phys.* **1965**, *12*, 1072.
(53) Wertheim, G. K.; Herber, R. H. *J. Chem. Phys.* **1963**, *38*, 2106.
(54) (a) Stukan, R. A.; Gubin, S. P.; Nesmeyanov, A. N.; Gol'danskii, V. I.; Makarov, E. F. *Teor. Eksp. Khim.* **1966**, *2*, 805. (b) Zahn, U.; Kienle, P.; Eicher, H., *Z. Phys.* **1962**, *166*, 220. (c) Birchall, T.; Drummond, I. *Inorg. Chem.* **1971**, *10*, 399.
(55) Ramadan, A. A.; Agasyan, P. K. *Zh. Obshch. Khim.* **1974**, *44*, 2299.
(56) Sohn, Y. S.; Hendrickson, D. N.; Gray, H. B. *J. Am. Chem. Soc.* **1971**, *93*, 3603.
(57) Duggan, D. M.; Hendrickson, D. N. *Inorg. Chem.* **1975**, *14*, 955, and references cited therein.
(58) Kramer, J. A.; Hendrickson, D. N., unpublished results.